Nonlinear Metamaterials with Multiple Local Mechanical Resonators: Analytical and Numerical Analyses

Mohammad Bukhari and Oumar Barry

Abstract This paper examines the role of stiffness nonlinearity on a periodic one-dimensional chain with multiple local resonators. The cells of the chain consist of lumped masses connected through nonlinear springs. Each cell is embedded with multiple local resonators having different parameters. In one case the local resonators are assumed to be linear and in another case they are nonlinear. The dispersion equation for the system is derived analytically by the method of multiple scales (MMS). The results are validated via comparison with those in the literature and numerically via Matlab. The nonlinearity shows enhancement in the bandgap regions, especially with increasing number of local resonators.

Keywords Acoustics metamaterial · Perturbation techniques · Wave propagation

1 Introduction

The study of metamaterials has gained lots of attention in recent years due to their exceptional material properties and characteristics and their wider engineering applications. Metamaterials are a new class of artificial composites that derive their unique dynamic properties from both engineered local configurations and material constituents [1]. They were originally developed for electromagnetic and optical wave propagation and later the technology was extended to acoustic and mechanical waves. Most if not all metamaterials required the presence of periodic features with the potential of exhibiting interesting dynamic phenomena such as resonance or instability within the host structure. These interesting dynamic features can be judiciously employed for suppressing noise and vibration, harvesting energy,

M. Bukhari (✉) · O. Barry
Department of Mechanical Engineering, Virginia Tech, Blacksburg, VA, USA
e-mail: bukhari@vt.edu; obarry@vt.edu

W. Lacarbonara et al. (eds.), *New Trends in Nonlinear Dynamics*,
https://doi.org/10.1007/978-3-030-34724-6_2

non-destructive testing structures for defects, improving image resolution, and ameliorating the performance of antennas and many other engineering structures and devices [3].

Numerous investigators have examined the linear behavior of metamaterials focusing on acoustic-induced vibration suppression. Some metamaterials can be represented as discrete or continuous systems with embedded local mechanical resonators consisting of mass-spring-damper systems. These mechanical locally resonant metamaterials exhibit bandgap formation at wavelengths much larger than the lattice size [2]. The bandgaps can be made wider by embedding multiple resonators inside the cells [4, 5]. Beyond their linear interesting properties, nonlinear metamaterials may show superior performance in terms of wave propagation properties [6]. The weakly nonlinear discrete periodic structures shift the dispersion curves. This shift may result in wider bandgaps associated with softening or hardening nonlinearity [7]. The derivation of nonlinear dispersion equations can be carried out using different perturbation techniques [8] such as the Lindstedt–Poincare or multiple scales techniques [9].

In this work, we study the effect of stiffness nonlinearity on one-dimensional wave propagation in a periodic structure (i.e., spring-mass chain) with multiple local resonators. The parameters of the local resonators are different in order to realize multiple bandgap formations. We investigate two different cases of nonlinearity: cubic spring nonlinearity connecting the chains and cubic spring nonlinearity in the local resonators. We also study both hardening and softening nonlinearities and investigate their roles on bandgap formations. Closed-form expressions are presented for the nonlinear dispersion equation for any number of local resonators. This is achieved using the method of multiple scales (MMS) to solve the weakly nonlinear system of governing equations of motion. The obtained expressions can serve as a benchmark for predicting the bandgap formations of weakly nonlinear acoustic metamaterials. This work also provides general guidelines for exploiting nonlinearity in order to achieve better vibration mitigation.

2 Derivation of the Dispersion Equation

Figure 1 shows a schematic diagram of the proposed nonlinear acoustics metamaterial that is represented by a chain of mass-spring systems with embedded local resonators. Each unit cell consists of a rigid mass, m, connected to other cells through linear and nonlinear spring coefficients, k, and $\epsilon\Gamma$, respectively. Inside each cell, there are multiple local resonators with a mass, m_i, and linear or nonlinear spring with linear coefficient, k_i, and nonlinear coefficient, $\epsilon\Gamma_i$. The nondimensional free oscillation equations for each cell with s number of local resonators can be expressed as

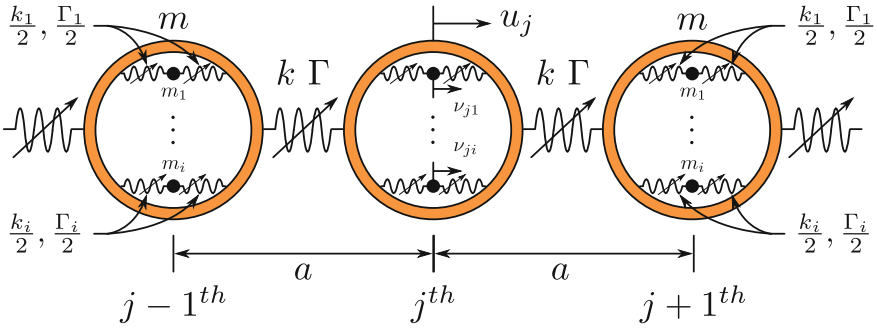

Fig. 1 The nonlinear acoustics metamaterial

$$\ddot{u_n} + 2u_n - u_{n-1} - u_{n+1} + \epsilon\bar{\Gamma}((u_n - u_{n-1})^3 + (u_n - u_{n+1})^3) + \sum_{i=1}^{s} \bar{k_i}(u_n - v_{ni}) + \sum_{i=1}^{s} \epsilon\bar{\Gamma_i}(u_n - v_{ni}) = 0 \tag{1}$$

$$\frac{\omega_n^2}{\omega_{di}^2}\ddot{v}_{ni} + (v_{ni} - u_n) + \epsilon\bar{\Gamma_i}(v_{ni} - u_n)^3 = 0, \tag{2}$$

where the dimensionless parameters are

$$\tau = \omega_n t; \bar{\Gamma} = \frac{\Gamma}{\omega_n^2 m}; \bar{k_i} = \frac{k_i}{\omega_n^2 m} \tag{3}$$

and ω_n and ω_{di} are defined as $\omega_n = \sqrt{k/m}$ and $\omega_{di} = \sqrt{k_i/m_i}$.

Using MMS, we can assume expansions for the displacements in the form of

$$u_n(t, \epsilon) = u_{n0}(T_0, T_1) + \epsilon\ u_{n1}(T_0, T_1) \tag{4}$$

$$v_{ni}(t, \epsilon) = v_{ni0}(T_0, T_1) + \epsilon\ v_{ni1}(T_0, T_1), \tag{5}$$

where $T_0 = \tau$ is the fast time scale and $T_1 = \epsilon\tau$ is the slow time scale. Since the time is expressed in two independent variables, the time derivative can be presented by using the chain rule as

$$(\ddot{}) = D_0^2 + 2\epsilon D_0 D_1 + \cdots, \tag{6}$$

where $D_n = \frac{\partial}{\partial T_n}$.

2.1 Nonlinear Chain

In this case, we are only interested to study the effect of spring nonlinearity connecting the cells (i.e., the case of nonlinear resonator is discussed in the next section since its dispersion relation is different from that of the nonlinear chain case). Consequently, we set $\bar{\Gamma}_i = 0$ (i.e., nonlinear springs in the local resonators are zero). Substituting Eqs. (4)–(6) into Eqs. (1)–(2) and collecting the similar coefficients of ϵ, one can get

Order ϵ^0

$$D_0^2 u_{n0} + 2u_{n0} - u_{(n-1)0} - u_{(n+1)0} + \sum_{i=1}^{s} \bar{k}_i (u_{n0} - v_{ni0}) = 0 \tag{7}$$

$$\frac{\omega_n^2}{\omega_{di}^2} D_0^2 v_{ni0} - (u_{n0} - v_{ni0}) = 0 \tag{8}$$

Order ϵ

$$\begin{aligned} &D_0^2 u_{n1} + 2u_{n1} - u_{(n-1)1} - u_{(n+1)1} + \sum_{i=1}^{s} \bar{k}_i (u_{n1} - v_{ni1}) \\ &= -2D_0 D_1 u_{n0} - \bar{\Gamma}((u_{n0} - u_{(n-1)0})^3 + (u_{n0} - u_{(n+1)0})^3) \end{aligned} \tag{9}$$

$$\frac{\omega_n^2}{\omega_{di}^2} D_0^2 v_{ni1} - (u_{n1} - v_{ni1}) = -2\frac{\omega_n^2}{\omega_{di}^2} D_0 D_1 v_{ni0}. \tag{10}$$

At order ϵ^0 the problem is linear; therefore, the solution can be expressed as

$$u_n = A e^{i(nk - \omega T_0)} + c \cdot c \tag{11}$$

$$v_{ni} = B_i e^{i(nk - \omega T_0)} + c \cdot c, \tag{12}$$

where $c \cdot c$ denotes complex conjugate, $k = qa$ is the dimensionless wave number, and q represents the wave number. A and B_i stand for the wave amplitude of the outer and inner masses, respectively. By substituting Eqs. (11)–(12) into Eqs. (7)–(8), the linear dispersion equation can be expressed as

$$-\omega^2 + (2 - 2\cos k) + \sum_{i=1}^{s} \bar{k}_i (1 - K_{\omega i}) = 0, \tag{13}$$

where $K_{\omega i} = \frac{1}{1 - \omega_n^2 \omega^2 / \omega_{di}^2}$. This linear dispersion equation represents both cases; however, the nonlinear dispersion relations are different. For nonlinear problem, we need to study the equations at order ϵ.

By rearranging the equations at order ϵ, we obtain

$$X(D_0^2 u_{n1} + 2u_{n1} - u_{(n-1)1} - u_{(n+1)1}) + \sum_{i=1}^{s} \frac{X\bar{k_i}\omega_n^2/\omega_{di}^2}{1-\omega_n^2\omega^2/\omega_{di}^2} D_0^2 u_{n1}$$
$$= -2\sum_{i=1}^{s} \frac{X\bar{k_i}\omega_n^2/\omega_{di}^2}{1-\omega_n^2\omega^2/\omega_{di}^2} D_0 D_1 v_{ni0} + X(-2D_0 D_1 u_{n0}$$
$$- \bar{\Gamma}((u_{n0} - u_{(n-1)0})^3 + (u_{n0} - u_{(n+1)0})^3), \tag{14}$$

where $X = \prod_{i=1}^{s}(\omega_n^2/\omega_{di}^2 D_0^2 + 1)$. Introducing Eqs. (11)–(12) into Eq. (14) yields

$$X(D_0^2 u_{n1} + 2u_{n1} - u_{(n-1)1} - u_{(n+1)1}) + \sum_{i=1}^{s} \frac{X\bar{k_i}\omega_n^2/\omega_{di}^2}{1-\omega_n^2\omega^2/\omega_{di}^2} D_0^2 u_{n1}$$
$$= \Bigg[2i\omega \sum_{i=1}^{s} \frac{X\bar{k_i}\omega_n^2/\omega_{di}^2}{1-\omega_n^2\omega^2/\omega_{di}^2} A' K_{\omega i} + X(2i\omega A'$$
$$-12\bar{\Gamma}A^2\bar{A}(1-\cos k)^2 \Bigg] e^{i(nk-\omega T_0)} + NST, \tag{15}$$

where NST denotes non-secular terms, $A' = \frac{dA}{dT_1}$, and $\bar{A}$ is the complex conjugate of A. We note here that X becomes $X = \prod_{i=1}^{s}(1-\omega^2\omega_n^2/\omega_{di}^2)$ after applying the operator D_0. The left-hand side of Eq. (15) has a nontrivial solution; therefore, the secular terms on the right-hand side must be eliminated by solving the solvability conditions [8] defined as the coefficients of $e^{i(nk-\omega T_0)}$.

Substituting the polar form $A = \frac{1}{2}\alpha e^{i\beta}$ into the solvability condition and separating the real and imaginary part, the modulation equations for the amplitude and phase can be expressed as

$$\omega \sum_{i=1}^{s} \frac{\bar{k_i} X\omega_n^2/\omega_{di}^2}{1-\omega_n^2\omega^2/\omega_{di}^2} \alpha' K_{\omega i} + X\omega\alpha' = 0 \tag{16}$$

$$-\omega \sum_{i=1}^{s} \frac{\bar{k_i} X\omega_n^2/\omega_{di}^2}{1-\omega_n^2\omega^2/\omega_{di}^2} \alpha\beta' K_{\omega i} - X\omega\alpha\beta' - \frac{3}{2} X\bar{\Gamma}\alpha^3(1-\cos k)^2 = 0. \tag{17}$$

From the amplitude equation above, one can find that α is constant (i.e., $\alpha = \alpha_0$). From the phase equation, we can obtain

$$\beta = -\frac{3\bar{\Gamma}\alpha^2(1-\cos k)^2}{2\omega\left(1 + \sum_{i=0}^{s} \frac{\bar{k_i}\omega_n^2/\omega_{di}^2}{1-\omega_n^2\omega^2/\omega_{di}^2} K_{\omega i}\right)} T_1. \tag{18}$$

Since $T_1 = \epsilon\tau$, the nonlinear frequency, ω_{nl}, associated with k is

$$\omega_{nl} = \omega + \epsilon\beta'. \tag{19}$$

2.2 Nonlinear Local Resonators

For this case, we are only interested in the nonlinearity from the local resonators hence we ignore the nonlinear spring coefficient of the cells (i.e., $\bar{\Gamma} = 0$). Following the techniques described in the previous section, one can express the phase as

$$\beta = -\frac{\sum_{i=1}^{s}\left[\frac{3}{8}\alpha^2(1-K_{\omega_i})^3\bar{\Gamma}_i\left(\frac{\bar{k}_i}{1-\omega_n^2\omega^2/\omega_{di}^2}-1\right)\right]}{\omega\left(1+\sum_{i=1}^{s}\frac{\bar{k}_i\omega_n^2/\omega_{di}}{1-\omega_n^2\omega^2/\omega_{di}^2}K_{\omega i}\right)}T_1. \tag{20}$$

Unlike the case of nonlinear chain, one should note here that the correction β is not explicitly a function of wave number. Moreover, the expression is different from that obtained in [10]. This is because the contribution of the resonators on the left-hand side from the equations at order ϵ was taken into account [6, 7].

3 Results and Discussion

For the numerical simulations, we select $\omega_0 = \omega_{d1} = 10^3$ for the case of single resonator. For the case of two local resonators we set $\omega_{d2} = 1.5\ \omega_0$ to obtain multiple bandgaps. The values of the nondimensional stiffness of the resonator are chosen to be $\bar{k}_i = \omega_{di}^2/\omega_0^2$. Also, the numerical simulation is based on $\epsilon\alpha^2\bar{\Gamma} = \epsilon\alpha^2\bar{\Gamma}_i = 0.06$. The band structure can be obtained by numerically integrating a chain (i.e., 100 cells were used in the simulation) excited at the middle (i.e., at $n = 50$) by a harmonic force. Then, we determine the wave number by picking the maximum value of the 2-D spectrum; such that the wave number is associated with the spatial frequency at the excitation frequency. Since the expression is derived for plane waves, the end condition is chosen to be a perfectly matched layer (PML); such that no reflected waves exist in the simulation. Following [9], this can be achieved by defining a linear viscous damping in the chain such as

$$c(n) = C_{\max}\left(\frac{n}{N}\right)^3, \tag{21}$$

where N is the number of simulated cells.

Figure 2a compares the results of the multiple scales method to those obtained using direct numerical integration, as well as, to those obtained in the literature using

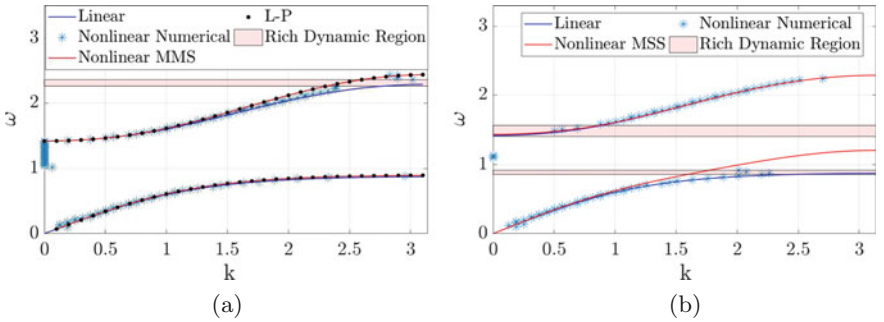

Fig. 2 Bandgap structure for single local resonator. (**a**) A chain connected by nonlinear spring. (**b**) Nonlinear resonators

Lindstedt–Poincare (L–P). The results show good agreement between the dispersion curves obtained by MMS and the results obtained by Lindstedt–Poincare (L–P) [6]. The comparison of the MMS results to the numerical results also shows a very good agreement in terms of detecting the boundaries of the bandgaps. But MMS fails to capture the rich dynamic region (i.e., inside the red patch), which is referred to pseudo-gap region [6]. It should be noted that pseudo-gap region here appears for different ranges as that observed in [6] because the input here is not wave packet. The wave indeed propagates through the structure, but the output appears at different multiple frequencies due to nonlinear interaction of the cells.

Figure 2b shows the analytical approximation (i.e., MMS) and numerical results of the band structure for the case of a single nonlinear local resonator. We can observe that the two methods slightly differ; particularly, when the frequency of the local resonator $\omega = \omega_{d1}$. Also, the comparison in terms of wider bandgap formation between nonlinear and linear local resonators is inconclusive in Fig. 2b. Higher order approximations or different analytical approximation methods such as the complexification averaging or the homotopy method may be required to obtain better accuracy and help provide better insight into the performance of the nonlinear local resonators.

Figure 3a shows the band structure of a chain connected by nonlinear springs with multiple local resonators. The results indicate that the MMS is a good predictor of the bandgap boundaries for multiple local linear resonators embedded in cells with nonlinear spring connections. The accuracy of the MMS approximation can even be further improved if higher order perturbation is considered. The results in this figure also show that the pseudo-gap almost vanishes; however, a narrow rich dynamic region still exists. For the case of multiple nonlinear local resonators, the same conclusion from Fig. 2b can be drawn. In that, Fig. 3b also reveals that the MMS is not very accurate in predicting the bandgap boundaries at frequencies confined between the resonators frequencies. The first order approximation of the MMS fails to predict the dynamic in the case of multiple nonlinear local resonators

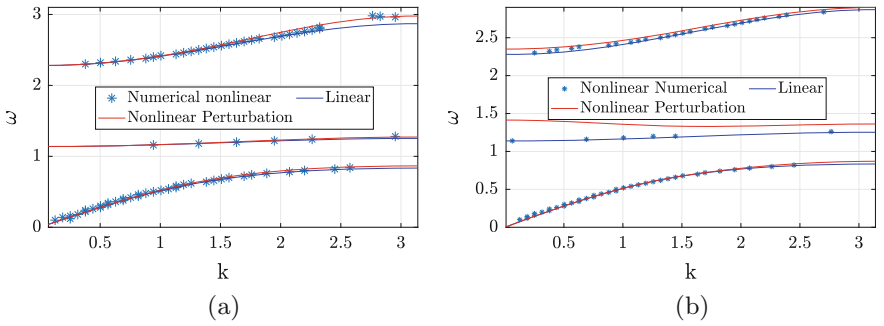

Fig. 3 Bandgap structure for two local resonators. (**a**) A chain connected by nonlinear spring. (**b**) Nonlinear local resonators

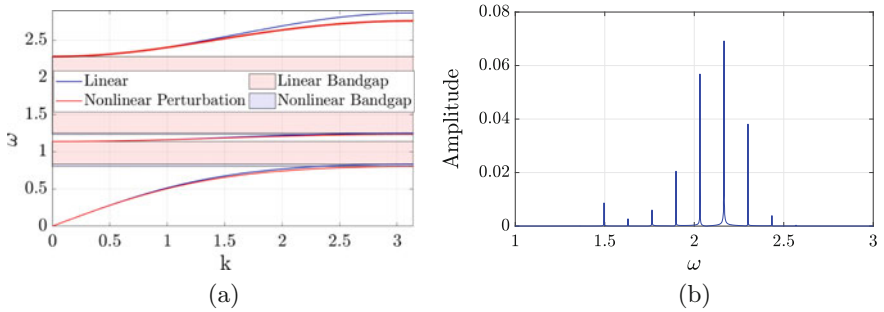

Fig. 4 Utilizing nonlinear chain toward vibration attenuation. (**a**) Softening nonlinearity. (**b**) Frequency shift

embedded in cells with linear spring connections. Hence, higher order perturbations or other analytical methods may be required to provide better approximations.

Finally, Fig. 4a shows that softening nonlinearity in the spring connecting the chain with multiple local linear resonators can be used to widening the bandgap. Therefore, the type of nonlinearity can be utilized in tuning the bandgap boundaries. Although softening nonlinearity is more desirable for vibration attenuation, solitary waves can only be realized with hardening nonlinearity [11]. In Fig. 4b, we can observe how the wave can appear at different secondary resonances due to softening or hardening nonlinearity. This frequency shift can be exploited in designing acoustics diode or acoustics rectifier [6, 12].

In the present study, we only handled the cubic type of nonlinearity. For other types of nonlinearities, one can approximate the nonlinearity by using Taylor expansion and rewrite the equation in terms of cubic polynomial. Similar procedures can then be used to derive the corresponding dispersion relations.

4 Conclusion

In this paper, we derived closed-form expressions of the dispersion equations describing the wave propagation in one-dimensional nonlinear acoustics metamaterial using the method of multiple scales. The obtained equations can be used in studying the dispersion curves for multiple local resonators unlike the one in the literature, which is limited to a single local resonator. The numerical simulations showed that these closed-form expressions accurately predict the band structure in the case of a chain with nonlinear spring connections and linear local resonators; whereas they fail to accurately predict the case of nonlinear local resonators embedded in cell with linear spring connection, particularly near the local resonator frequency. Numerical examples also demonstrate that wider forbidden regions can be achieved with multiple local resonators. This is an indication that superior vibration mitigation can be realized by the proposed softening or hardening nonlinearity.

Acknowledgement The authors would like to thank Mr. David Petrushenko for his help in generating figures and the start-up funding provided by Virginia Tech.

References

1. Hussein, M.I., Leamy, M.J., Ruzzene, M.: Dynamics of phononic materials and structures: historical origins, recent progress, and future outlook. Appl. Mech. Rev. **66**(4), 040802 (2014)
2. Liu, Z., Zhang, X., Mao, Y., Zhu, Y.Y., Yang, Z., Chan, C.T., Sheng, P.: Locally resonant sonic materials. Science **289**(5485), 1734–1736 (2000)
3. Bertoldi, K., Vitelli, V., Christensen, J., van Hecke, M.: Flexible mechanical metamaterials. Nat. Rev. Mater. **2**(11), 17066 (2017)
4. Huang, G.L., Sun, C.T.: Band gaps in a multiresonator acoustic metamaterial. J. Vib. Acoust. **132**(3), 031003 (2010)
5. Zhu, R., Liu, X.N., Hu, G.K., Sun, C.T., Huang, G.L.: A chiral elastic metamaterial beam for broadband vibration suppression. J. Sound Vib. **333**(10), 2759–2773 (2014)
6. Zhou, W.J., Li, X.P., Wang, Y.S., Chen, W.Q., Huang, G.L.: Spectro-spatial analysis of wave packet propagation in nonlinear acoustic metamaterial. J. Sound Vib. **413**, 250–269 (2018)
7. Narisetti, R.K., Leamy, M.J., Ruzzene, M.: A perturbation approach for predicting wave propagation in one-dimensional nonlinear periodic structures. J. Vib. Acoust. **132**, 031001 (2010)
8. Nayfeh, A.H.: Introduction to Perturbation Techniques. Wiley, New York (2011)
9. Manktelow, K., Leamy, M.J., Ruzzene, M.: Multiple scales analysis of wave-wave interactions in a cubically nonlinear monoatomic chain. Nonlinear Dyn. **63**, 193–203 (2011)
10. Kulkarni, P.P., Manimala, J.M.: Nonlinear and inertant acoustic metamaterials and their device implications. In: Dynamic Behavior of Materials, vol. 1, pp. 217–234. Springer, Cham (2018)
11. Ganesh, R., Gonella, S.: Spectro-spatial wave features as detectors and classifiers of nonlinearity in periodic chains. Wave Motion **50**(4), 821–835 (2013)
12. Ma, C., Parker, R.G., Yellen, B.B.: Optimization of an acoustic rectifier for uni-directional wave propagation in periodic mass-spring lattices. J. Sound Vib. **332**(20), 4876–4894 (2013)